Beet curly top Iran virus Rep and V2 gene work as silencing suppressors through separate mechanisms

Saeideh Ebrahimi[1,2], Alexandra Baßler[1], Omid Eini[2,3], Zeynep Yildirim[1], Michael Wassenegger[1], Gabi Krczal[1], Veli Vural Uslu[1,4,*]

[1] RLP AgroScience GmbH, Breitenweg 71, 67435, Neustadt an der Weinstraße, Germany
[2] Department of Plant Protection, University of Zanjan, 313 Zanjan, Iran
[3] Department of Phytopathology; Institute for Sugar Beet Research; 37079 Göttingen, Germany
[4] MAPS, Heidelberg University, Heidelberg, Germany

**Corresponding author: velivural.uslu@agroscience.rlp.de*

Abstract

Beet curly top Iran Virus (BCTIV) is a yield-limiting geminivirus belonging to the *becurtovirus* genus. The genome organization of BCTIV is unique in a way that the complementary strand of BCTIV resembles mastreviruses, whereas the virion strand organization is close to curtoviruses. Geminiviruses are known to avoid the plant defense system by suppressing the RNA interference mechanisms both at the transcriptional gene silencing (TGS) and post-transcriptional gene silencing (PTGS) level. Multiple geminivirus genes have been identified as viral suppressors of RNA silencing (VSR) but the genes underlying VSR activity remain elusive in becurtoviruses. We performed an unbiased screen on each individual BCTIV gene for VSR activity based on three different PTGS experimental setups with transient silencing inducers on stably GFP-expressing *Nicotiana benthamiana* (16C) and on transiently GFP expressing wild-type *Nicotiana benthamiana* (WT). We found that only V2 and Rep were able to suppress specific PTGS mechanisms. BCTIV-V2 could suppress S-PTGS more efficiently than BCTIV-Rep when there is transient GFP expression. However, Rep but not V2 could suppress S-PTGS when GFP is only stably expressed by 16C. Furthermore, neither V2 nor Rep could suppress local PTGS induced by inverted repeat targeting GFP (GFP-IR) when GFP is only stably expressed by 16C. Nevertheless, Rep suppressed the systemic silencing induced by GFP-IR in 16C plants. BCTIV-Rep inhibits silencing by mitigating sRNA production, whereas BCTIV-V2 does not alter sRNA, suggesting that Rep and V2 have distinct modes of action. Further characterization of BCTIV-Rep by deletional mutagenesis implicated that multiple domains are required for silencing suppressor activity of Rep. This is the first study revealing the genes responsible for silencing suppression in a becurtovirus and implicating their mode of action.

Introduction

Beet curly top Iran virus (BCTIV) has a monopartite single-stranded DNA (ssDNA) genome and belongs to *becurtovirus* genus of the *geminiviridae* family (Heydarnejad, Keyvani et al. 2013). BCTIV is a yield-limiting virus, causing a serious leaf curl disease in economically important crops such as sugar beet, tomato, pepper and beans (Yazdi et al 2008, Heydarnejad et al 2013).The leaf curl symptom induced by BCTIV is very similar to those caused by other members of the geminiviridae, such as beet curly top viruses (BCTV) of curtovirus genus (Anabestani et al 2017). However, BCTIV transmission relies on a distinct vector, *Circulifer haematoceps* (Taheri et al 2012) and the genome organization of BCTIV differs from the other members of the *geminividae* (Yazdi et al 2008). Yet the functions of the BCTIV encoded proteins have not been addressed rigorously.

Geminiviruses encode four to eight proteins in their mono- or bi-partite genomes. The transcription from the geminivirus genome takes place in a bidirectional fashion: complementary strand (C) and virion strand (V) (Teixeira et al. 2021). Geminiviruses contain a TAGTATTAC sequence at the replication origin (*ori*), where the replication is initiated by the viral replication initiator protein, known as the complementary strand protein 1 (C1) (Teixeira et al. 2021). Other proteins in the complementary strand are transcriptional activator protein C2, replication enhancer protein C3, pathogenicity determinant proteins C4 and C5 (Kumar 2019). In addition, in *mastrevirus*, *capulavirus*, *grablovirus* genus, due to a splicing event between C1 and C2, a new open reading frame, called Rep, emerges containing the N terminus of C1 and a frame-shifted C terminus of C2. Rep protein of geminiviruses is a multifunctional protein which is indispensable for viral genome replication (Ruhel and Chakraborty 2019). On the other hand, the virion strand encodes the coat protein (V1), movement protein (V2), and a poorly characterized gene (V3) (Kotlizky et al 2000). The C and V genes are organized in unique combinations for each genus of geminiviridea family. For example, BCTIV contains C1, C2, and Rep on the complementary-sense strand, similar to Mastreviruses, whereas V1, V2 and V3 on the virion-sense strand, similar to curtoviruses (Bozorgi et al. 2017) (Supplementary Figure 1a).

One critical aspect of the geminivirus pathology is that the efficiency of virus accumulation depends on the suppression of RNA interference (RNAi) in plants (Hanley-Bowdoin et al. 2013). RNAi is a conserved mechanism, acting through transcriptional (TGS) or post-transcriptional (PTGS) repression of gene expression in a sequence-specific manner (Baulcombe 2004). One of the vital functions of RNAi is to protect plants against pathogens, including viruses. RNAi in plants is triggered by double stranded RNA (dsRNA). dsRNA is cleaved into small RNAs (sRNAs) of distinct lengths by Type III endonucleases, called DICER-LIKE (DCL) proteins (Baulcombe 2004). sRNAs are incorporated into ARGONAUTE (AGO) proteins and form the RNA-induced silencing complex (RISC) for the cleavage of the target sequence, recruitment of RNA dependent RNA polymerase (RDRs), or facultative inhibition of translation. In addition to the core components of RNAi, auxiliary proteins like HUA

ENHANCER 1 (HEN1) RNA methyltransferase by protecting sRNAs from degradation, and SUPPRESSOR OF GENE SILENCING 3 (SGS3) and SILENCING DEFECTIVE 5 (SDE5), by facilitating RDR activity, contribute to RNAi and viral defense in plants (Cheng and Wang 2017)

There are many identified viral TGS and PTGS suppressors in plant viruses. For example, helper component-proteinase (HC-Pro) encoded by *Potyviridae* inhibits RDR6 (Zhang et al. 2008) and HEN1 (Jamous et al. 2011) among other components of RNAi pathway, whereas, P19 protein (P19) of *Tomato bushy stunt virus* sequesters ds-siRNAs inhibiting RNAi based protection in plants (Voinnet et al. 2003, Ye et al. 2003). In addition, the P6 protein of *Strawberry vein banding virus* (Feng et al. 2018), the P20, P23 and capsid proteins of *Citrus tristeza virus* (Lu et al. 2004), the P6 protein of *Cauliflower mosaic virus* (Haas et al. 2008), P38 protein of *Turnip crinkle virus* (Iki et al. 2017), P1 of *Sweet potato mild mottle virus* (Giner et al. 2010) are among those, which are have been shown to function as viral suppressors of RNA silencing (VSR). In *Geminiviridae*, several reports have implicated that C2, C4, C5, Rep, V2 and V3 proteins (Liu et al. 2014, Wang et al. 2014, Hanley-Bowdoin et al. 2013) function as viral VSRs, involved in suppression of transcriptional gene silencing (TGS) or post-transcriptional gene silencing (PTGS) in plants. Yet, the silencing suppressor activity of the BCTIV gene products remains elusive.

In this study we performed an unbiased screen on all BCTIV genes for their possible role as a suppressor of PTGS in local and systemic context and addressed their mode of action.

Materials and Methods:

Plasmid constructs for transient expression

Sense-PTGS silencing inducers were cloned into pGreen (pG104) vector containing full length (FL-GFP) or only 139nt long 5´-GFP sequence (5´-GFP) (Dalakouras et al. 2019). Strong PTGS was induced by the inverted repeat of the very same 139nt sequence (GFP-IR) with a 90nt long spacer as described in Dalakouras et al. 2019. The positive VSR control P19 of TBSV was expressed in pPCV702SM binary vector (Saeed et al 2015). All silencing inducers are expressed under the control of 35S promoter.

For unbiased investigation of the genes potentially responsible for VSR, all the predicted and verified ORFs of BCTIV (C1, C2, C4, C5, Rep, V1, V2, V3, V4) in pDIVA and/or pG104 binary vectors (Ebrahimi et al 2022) were examined on 16C plants. The coding sequences of the C1, C2, Rep and V2 genes were amplified with primers with BamHI and XhoI restriction cut sites (Table 1), using Q5 polymerase (NEB). The PCR products were first cloned into pJET1.2/blunt cloning vector (Thermo Fischer Scientific, Germany) and they were sub-cloned into *Xho*I and *BamHI* sites of pG104 vector to obtain pG-C1, pG-C2, pG-Rep and pG-V2, to obtain the same vector backbone for all silencing inducers. The inserts were confirmed by Sanger-sequencing. Of note, we found out that the vector backbone did not influence the silencing or VSR phenotypes.

12 truncations from Rep gene were amplified using corresponding primers (Table1) and then digested with the BamHI and XhoI enzymes. First, they were inserted into pJET1.2 (above) plasmid and after sequencing were cloned into pG104 vector to obtain pG-Rep1, pG-Rep2, pG-Rep3, pG-Rep4, pG-Rep5, pG-Rep6, pG-Rep7, pG-Rep8, pG-Rep9, pG-Rep10, pG-Rep11 and pG-Rep12.

Escherichia coli (strain INVαF, ThermoFisher) was used for cloning plasmid constructs and *A. tumefaciens* strain ATHV was used for transient transformation of the plants. pSoup helper plasmid was used together with pG104 for transforming agrobacterium by electroporation. In addition to the plasmid constructs obtained from INVαF, plasmids in the *agrobacterium* clones were also sequenced to ensure the insert integrity.

Agroinfiltration

The BCTIV genes were co-infiltrated with *Agrobacterium* ATHV containing silencing inducer constructs into wildtype *Nicotiana benthamiana* (WT) and GFP-expressing *N.benthamiana* (16C) at four-leaf-stage. *Agrobacteria* containing the constructs were grown in LB medium (containing Kanamycin and Rifampicin) at 28.0 °C for 16 h with continuous shaking at 135 rpm, then re-suspended in MES buffer (10 mM MgCl2, 10 mM MES (pH 5.6), and 100 µM acetosyringone) to reach OD_{600}= 1 For agroinfiltration. For negative control, *N. benthamiana* plants were separately infiltrated with FL-GFP, 5´-GFP and GFP-IR. In order to equalize the strength of silencing induction in single silencing inducer infiltrations, agrobacterium containing empty pG104 (OD_{600}= 1) has been added for mock co-infiltrations.

Unless otherwise stated, six plants were used for each treatment in each experiment, and each experiment was repeated at least three times at different times of the year to avoid any effect of temperature fluctuations in the greenhouse.

GFP imaging and quantification

The inoculated plants were maintained in a growth chamber at 25 °C with 16-h light/ 8-h dark period. After 3 days post inoculation (dpi) the control plants were monitored regularly under UV light (Blak-Ray B-100 AP Lamp, www.uvp.com) to visualize the silencing phenotype. At 6dpi all the plants were recorded using a Canon camera (Canon EOS700D, 18-5mm Lens) under UV light and leaves were scanned using a laser scanner (Molecular Imager® PharosFX™ Systems, BioRad) at 50µm per pixel, in GFP (excitation at 488nm, emission at 530nm) and in Chlorophyll (excitation at 488nm, emission at 695nm) channels.

The GFP and the Chlorophyll images were merged and then GFP expression was quantified in the limited area of infiltrated patches. GFP expression was measured by FIJI image analysis in nine spots

on treated, non-necrotic area and the acquired values were normalized using non treated areas (www.imagej.net). The final values were plotted in bar charts (BoxPlotR, Shiny Lab).

Protein Extraction and Western blot

Total protein was extracted from 6 dpi infiltrated leaf patches of WT plants using protein extraction buffer (1M Tris-HCl, PH 8.8, 10% Glycerol, 10% SDS and H2O) together with cOmplete™ Protease inhibitor solution (Roche). SDS-PAGE was performed for Coomassie staining and Western blotting (Wb), SicGen polyclonal goat anti-GFP antibody (AB0066-200, 1:1000) as primary, Donkey anti-goat IgG antibody (1:5000) as secondary antibody were used for western blot. Pierce™ ECL Western Blotting Substrate (ThermoFisher) was used to detect the signal. In the experiment set up, 16C *N.benthamiana* were not included for the western blot analysis due to the fact that the vasculature of 16C is barely affected by silencing, and depending on how much vasculature is included in the western blot sample collection from silenced areas, the results fluctuate dramatically.

RNA extraction, RT-PCR and Northern blot

Total RNA was extracted from infiltrated patches of 16C leaves at 6 dpi using TRIzol® Reagent (Qiagen). RNA concentration and RNA purity were measured using Nanodrop (ND-1000) and RNA quality was assessed by agarose gel electrophoresis. RT-PCR was performed using the SuperScript™ III One-Step RT-PCR System with Platinum™ Taq DNA Polymerase (Invitrogen™, ThermoFisher) and gene specific primers to amplify BCTIV genes to confirm transient expression of the constructs upon agroinfiltration. For Northern blot of GFP mRNA and GFP siRNA 10μg and 5μg of total RNA were used, respectively, as previously described (Dalakouras et al. 2019). The siRNA Northern blots were stripped and rehybridized with a U6 snoRNA probe. For GFP probes [alpha-P32] CTP is used for labeling, for U6 snoRNA probe [gamma-p32] ATP is used from Hartman Analytic, Germany. The detection of the Northern blot signals was performed by the Molecular Imager® PharosFX™ Systems (BioRad).

Results

Phenotypic analysis of BCTIV genes on *N. benthamiana*

Initially, we conducted a screen to monitor the effect of the BCTIV genes on 16C *N. benthamiana*. C1, C2, Rep, V1, V2, and V3 genes, which were previously shown to be expressed by BCTIV and potential C4, C5, and V4 ORFs, for which it is still unclear whether they are expressed upon BCTIV infection or not (Supplementary Figure 1a) (Eini et al 2016, Yazdi et al 2008). First of all, we verified the expression of the viral genes in *N. benthamiana* leaves using RT-PCR (Supplementary Figure 1b). Our initial test on 16C plants showed that transient expression of C2, V1, V2, and V3 produced no

visible phenotype, whereas C4 and C5 displayed a very strong necrotic phenotype especially in older leaves as early as 5dpi (data not shown). C1 and Rep expression also led to necrotic speckles starting from 5dpi and the necrotic phenotype gradually got stronger. As sense-PTGS (S-PTGS) inducer, 5'-GFP construct was agroinfiltrated into GFP expressing 16C leaves. The silencing phenotype induced by 5'-GFP was most consistently visible from 6dpi on (data not shown). Therefore, we assessed the effect of BCTIV genes on local S-PTGS at 6dpi.

BCTIV-Rep suppresses local sense-PTGS in *N.benthamiana*

Initially we aimed at investigating the role of BCTIV genes in S-PTGS pathway. For this assay, 139nt long sequence mapping to GFP (5'-GFP) was transiently expressed together with the BCTIV genes in 16C *N. benthamiana*. Due to S-PTGS induction, agroinfiltrated leaf sectors turn red under the UV light due to loss of GFP at 6dpi. However, if a BCTIV gene functions as viral suppressor of RNA silencing (VSR) the agroinfiltrated sector remains green under the UV light (Figure 1a). Based on the GFP expression level under the UV light at 6 dpi, we found out that only Rep protein could suppress the S-PTGS, while none of the other constructs, including the positive control TBSV-P19, could suppress S-PTGS (Figure 1b). For the exact quantification of GFP levels after silencing induction and silencing suppression, the leaves were imaged in high resolution laser scanner (Figure 1c). The GFP intensity measurements in exclusively non necrotic areas showed that GFP expression was significantly ($P < 0.05$) higher in Rep infiltrated 16C *N. benthamiana* leaves in comparison to TBSV-P19 and other BCTIV gene infiltrations plants. (Figure 1d).

To reveal the mode of action of VSR activity of BCTIV-Rep, we investigated the GFP mRNA and small RNA populations upon co-infiltration in the leaf sections of 16C plants using Northern blot. To compare with Rep, we used a restricted set of BCTIV-genes, including C1 and C2 because of overlapping sequences with Rep, and V2 genes due to the VSR activity of V2 homologues in other geminiviruses (Luna et al 2017, Zhang et al 2012, Zrachya et al 2006). Despite loading same amounts of material according to nanodrop measurements, the RNA quality of different co-infiltrations differed a lot based on rRNA bands on the agarose gel electrophoresis of the RNA samples. Especially, due to the necrotic areas caused by Rep, the RNA integrity was the lowest in Rep + 5´-GFP co-infiltrated sample. Nevertheless, the GFP mRNA level in Rep + 5´-GFP was the highest when compared to other co-infiltrated samples and only 5´-GFP infiltrated silenced material (Figure 1e). Moreover, GFP mRNA level in Rep+5´-GFP is only slightly lower than non-treated 16C leaf control.

In addition, we performed sRNA Northern Blot on the very same co-infiltrated samples. End labelled U6 snoRNA probe was used as a loading control, which did not reveal any major fluctuations of sRNA concentration (Figure 1f). samples from untreated 16C did not show any sRNAs and 5´-GFP treated 16C samples had clear accumulation of sRNAs, suggesting that the experimental set up was valid. Rep

+ 5´-GFP sample showed only a very faint sRNA bands at the level of 21-24 nucleotides (nt), suggesting that Rep interfered with silencing pathway, before the production of sRNAs by DCLs (Figure 1f). P19 and V2 co-infiltration with 5´-GFP lead to only limited decrease in sRNA production in concordance with the previous literature (Saeed et al 2015).

BCTIV-V2 suppresses local S-PTGS only when the GFP is transiently expressed.

In order to detect the changes in GFP expression and silencing levels in a clean background with no GFP fluorescence over the whole leaf surface, full-length GFP (GFP-FL) was co-infiltrated together with BCTIV-genes in wt *N. benthamiana*. GFP-FL under the control of 35S promoter induces GFP expression. However, due to the S-PTGS mediated self-silencing of the transient GFP-FL expression, the GFP signal remains low. When a BCTIV gene increases the GFP expression, upon co-infiltration with GFP-IR, this is due to the VSR activity of the gene, which inhibits S-PTGS, hence, the self-silencing of GFP-FL (Figure 2a).

Plants under the UV light at 6 dpi showed high GFP expression in the BCTIV-V2 and BCTIV-Rep treated plants compared to only GFP-FL infiltrated plants (Figure 2b). The strongest green fluorescence was observed in TBSV-P19 treated plants, in accordance with the previous literature (Figure 2b) (Ahn et al. 2011, Saeed et al 2015, Zhang 2015). The quantification based on high resolution images of infiltrated leaves also corroborated with the observations under the UV lamp, in which P19, V2, and Rep showed higher GFP signal than the GFP-FL only and GFP-FL with C1 or C2 (Figure 2c, d).

Since wt plants provided a blank background for GFP analysis, we addressed whether the quantifications on the images based on GFP intensity in non-necrotic areas matched with the GFP amount in the non-necrotic areas obtained by Western blot on the carefully dissected infiltrated areas. Western Blot results also showed that co-infiltration of GFP-FL with P19, V2, and Rep led to higher GFP protein expression than GFP-FL alone at 6dpi, in the same order of intensity (Figure 2e). Moreover, C1 and C2 co-infiltration with GFP-FL did not increase the GFP protein level in Western blot in accordance with the image analysis.

We performed the GFP-FL co-infiltration with P19, V2, and Rep on GFP expressing 16C *N.benthamiana*. GFP-FL is increases GFP expression but also functions as S-PTGS inducer in the later stages. At 5.25dpi, we found out that the net contribution of GFP-FL on the GFP level is zero (Figure 2f, g). At this stage, P19 works as a silencing suppressor, more efficiently than V2. Although V2+GFP-FL tends to have stronger silencing suppressor effect than Rep+GFP-FL in average, the difference is not statistically significant (Figure 2g).

Neither Rep nor V2 can suppress PTGS induced by a hairpin construct targeting GFP.

Since Rep is capable of decreasing sRNA production, necessary for S-PTGS, we addressed whether Rep can repress PTGS induced by hairpin RNA (GFP-IR) expressed under the control of 35S promoter. Similar to the S-PTGS infiltrations using GFP-FL and 5´GFP, the same agrobacterium batch containing BCTIV genes (C1, C2, Rep and V2) were co-infiltrated with GFP-IR in stably GFP expressing 16C plants (Figure 3a). GFP-IR is a very strong inducer of silencing and at 6dpi, none of C1-, C2-, Rep-, V2-, P19- co-infiltrated leaves showed loss of the silencing phenotype (Figure 3b). Nevertheless, C1 and Rep co-infiltrated with GFP-IR had a slightly higher level of GFP than GFP-IR only (Figure 3c, d). Therefore, we investigated the molecular fingerprints of BCTIV genes on PTGS by checking GFP mRNA and sRNA levels using Northern blot on stably GFP expressing 16C plants.

Due to lower necrotic areas in Rep + GFP-IR sample, the RNA quality was comparable to the other treatments and controls. In addition, the abundance of GFP mRNA in 16C and the low level of GFP in GFP-IR treatment validated the experimental set up. None of the treatments, including Rep, could block the decrease of GFP mRNA level upon GFP-IR induction (Figure 3e).

Next, we have performed a sRNA Northern blot. U6 snoRNA loading control shows comparable amounts of total sRNAs among different treatments and controls (Figure 3f). In addition, GFP-IR only shows very strong sRNA accumulation, whereas no sRNAs are visible in 16C control, validating the experimental set-up. Interestingly, we have seen that the population of sRNAs mapping to GFP is almost absent in Rep + GFP-IR and dramatically reduced in C1+GFP-IR at 6dpi. The V2 and P19 co-expression with GFP-IR did not have any effect on sRNA accumulation at 6dpi (Figure 3f).

Rep but not V2 can suppress systemic silencing

To find out whether the decrease in sRNA amounts upon expression of BCTIV genes suppresses systemic silencing in 16C plants (Figure 3f), the GFP-IR treated plants were observed and recorded regularly under the UV light until 14dpi (Figure 3g). Systemic silencing emerged at 10 dpi in plants infiltrated with GFP-IR only, upon C2+GFP-IR and V2+GFP-IR co-infiltration the systemic silencing phenotype spread in the new emerging leaves at 14 dpi, without any exception (Figure 3g, h). None of the eighteen plants infiltrated with Rep+GFP-IR showed systemic silencing, however (Figure 3h). These results indicate Rep protein suppression activity in systemic PTGS. It is noteworthy that twelve out of eighteen C1+GFP-IR treated plants did not show any systemic silencing and the remaining six out of eighteen plants showed rather restricted systemic spread of the silencing signal (Figure 3g, h).

Rep and V2 do not interfere with the spread of silencing through plasmodesmata

Local silencing induced by GFP-IR and/or GFP-FL creates a visible area encircling the infiltration zone, which shows stronger silencing than the infiltration zone (Figure 4a, Himber et al 2003). It is postulated that the silencing signal reaches to this area via the short-range spreading of sRNAs through

plasmodesmata (Dunoyer et al. 2005, Kalantidis et al. 2008). It is possible to quantify the length and GFP intensity (Gray value) of this area by plotting the profile (using FIJI) along a line in GFP channel. Our data showed that the GFP-IR+GFP-FL co-infiltration created a silenced zone of 0.635mm around the infiltration zone, which roughly corresponds to 15 cells (Figure 4b). When GFP-FL, GFP-IR are co-infiltrated with p19, V2 or Rep on 16C *N.benthamiana*, the silencing phenotype is partially and significantly repressed at 5.25dpi (Figure 4c, e, g, i). While, P19 abolishes the silenced ring around the infiltrated area, the area is preserved when BCTIV-V2 and BCTIV-Rep are co-infiltrated with the silencing inducers (Figure 4d,f,g).

Multiple Rep domains are indispensable for VSR activity

To figure out if there is any specific domain responsible for suppression activity in Rep protein, different truncations of Rep gene were constructed based on C1 and frameshift C2 motifs (Supplementary Fig 2). The obtained truncations were co-expressed together with 5´-GFP in 16C *N. benthamiana* plants (Figure 5a). None of the 12 Rep truncations demonstrated suppression activity at 6dpi (Figure 5b) which correlates with GFP quantification in infiltrated leaf patches (Figure 5c,d). Interestingly a subset of Rep truncations constructs showed necrotic phenotypes similar to Rep induced phenotypes which demonstrates that the N-terminus but not the C-terminus of the Rep protein is responsible for necrosis induction, which is different from its suppression activity, partially overlapping with the Rep truncations in wheat dwarf virus (WDV) (Liu et al. 2014)

Discussion

RNA silencing is a cellular defense mechanism conserved across kingdoms which is triggered by ds-RNA in plants (Zhao *et al*., 2022). Geminiviruses, in spite of being ssDNA viruses with no dsRNA phase in their replication cycle, have been shown to be targeted by plants via post-transcriptional gene silencing, probably by producing bi-directional transcription from opposite polarity or the strong fold-back structure of transcripts (Vanitharani et al., 2005). Therefore, Geminiviruses must confront both transcriptional (TGS) and posttranscriptional gene silencing (PTGS) to achieve successful infections (Luna et al., 2017). Several open reading frames were identified as TGS and PTGS suppressors in Geminiviruses but still, there is no report of silencing suppressors in BCTIV. In this study we used distinct approaches to dissect the role of BCTIV genes in the suppression of PTGS.

First of all, when the GFP-FL is agroinfiltrated on WT plants, it induces GFP expression but also due to accumulation of aberrant RNAs, triggering S-PTGS it silences itself subsequently (Parent et al. 2015). When GFP-FL is transiently expressed, we showed that BCTIV-V2 works as an effective silencing suppressor showing overlapping features with TBSV-P19 VSR activity. In this context, Rep

also represses the self-silencing of FL-GFP but only very mildly. However, when the GFP is solely expressed in the genome in 16C *N. benthamiana* (without transient GFP-FL expression) and the S-PTGS is induced by transient expression of 5´-GFP, TBSV-P19 and BCTIV-V2 have no repressive effect on silencing in our experiments, whereas BCTIV-Rep completely suppresses the S-PTGS in this context. The Northern blots of leaves in which S-PGTS was induced by infiltration with 5´-GFP, TBSV-P19, and BCTIV-V2 co-infiltrated samples showed accumulation of sRNAs, whereas BCTIV-Rep co-infiltrated sample was almost fully devoid of sRNAs. The sRNA signature indicates that P19 and V2 do not interfere with the sRNA production substantially. On the other hand, Rep interferes with sRNA production. These observations implicate that BCTIV-Rep has a distinct mechanism of action from BCTIV-V2 and TBSV-P19.

GFP-IR is indeed a very strong silencing inducer, which can lead to systemic silencing within 10 dpi. Upon transient expression of GFP-IR a hairpin structure, which maps to the GFP transcript, dsRNA immediately form and is subsequently processed by the DCL proteins. In this situation, none of the silencing suppressors, including Rep could repress the local silencing induced by GFP-IR. Nevertheless, the sRNA Northern blot showed that Rep and C1 could decrease the amount of sRNAs produced upon GFP-IR expression. Although the decrease did not lead to suppression of local silencing, the systemic silencing phenotype was consequently affected. On the other hand, V2 did not have any effect on the systemic silencing. It has recently been proposed that the AGO proteins sequester the sRNAs and mobile sRNAs can induce systemic silencing only when their concentration is above a certain threshold, determined by the concentration of AGO proteins (Vionnet 2022). Therefore, the reduction in sRNA level by Rep which does not affect local silencing is low enough to avoid induction of systemic silencing. Besides, it is worth mentioning that the necrotic phenotype of the Rep and C1 could further decrease the production of sRNAs after 6dpi, which contributes at least partly to the lack of systemic silencing phenotype in these co-infiltrations.

Nevertheless, it was still puzzling that P19 did not lead to any silencing suppression when 5´-GFP or GFP-IR was expressed on stably GFP expressing 16C plants (Supplementary Figure 3a, b). Vast majority of the characterization of the P19 activity was performed under transient expression of GFP in 16C or WT backgrounds (Martin-Hernandez and Baulcombe, 2008). Confirming the previous literature, when GFP was transiently expressed, we could recapitulate the silencing suppression phenotype of p19 (and V2) on WT or 16C plants (Vargason et al. 2003, Silhavy et al. 2002) (Supplementary Figure 3c-f).

The underlying mechanism of the VSR activity of p19 and V2 on S-PTGS depending on the presence of transient GFP-FL expression remains enigmatic (Supplementary Figure 3a-f). In order to understand the phenomenon, we transiently expressed P19 two and one day before the GFP-IR expression on 16C

samples. In three independent experiments, we consistently found out that P19 can act as a silencing suppressor in the absence of GFP-FL, if it is expressed not one day but at least two days before the silencing inducer GFP-IR or 5'-GFP is expressed on 16C plants (Supplementary Fig 4a-e). On the contrary, although p19 suppresses silencing when co-infiltrated with GFP-FL, when GFP-FL is expressed one or two days before p19, p19 cannot suppress the silencing (Supplementary Figure 4f-i). It has previously been demonstrated that P19 binds to ds-siRNA to inhibit the silencing derived from ds-siRNA (Liu et al., 2012). Also in line with P19-binding specificity, P19 failed to inhibit the activation of RISC by ss siRNA, similarly, P19 was not able to suppress the target cleavage of the already activated RISC (Lakatos et al., 2004). Furthermore, another study showed CymRSV infection was not able to revert the already established GFP RNA silencing. (Silhavy et al., 2002). To sum up, our experiments as well as the given literature indicate that the time of p19 expression relative to the GFP-FL is critical for its function. The difference in timing may create a difference in p19 and siRNA concentrations at a given time, which is critical for the VSR activity.

Although this is the first report of silencing suppressor gene of BCTIV-Rep protein, Rep was previously identified for as a PTGS suppressor in different geminiviruses like *Wheat dwarf virus* (WDV) from *Mastrevirus* (Kasschau and Carrington 1998, Liu et al. 2014). Yet, BCTIV-Rep protein is only very distantly related to WDV-Rep proteins based on amino acid sequence (Supplementary Figure 5). Therefore, the precise identification of the RNAi pathways that Rep proteins involve in may shed light on uncharted functions of Rep proteins in geminiviruses. For example, Rep protein from TYLCV, TGMV, ACMV was shown to interfere with the plant DNA methylation machinery and suppresses transcriptional gene silencing (Rodríguez-Negrete et al. 2013), which we did not observe for BCTIV-Rep (data not shown). In addition, V2 and its homolog AV2 have previously been identified as a suppressor in Geminiviruses, with a weaker silencing outcome than p19 (Sharma et al., 2010), but it had not been reported for BCTIV before this study.

In contrast to the suppression mechanism by V2 and TBSV-P19, we propose that BCTIV-Rep protein interferes with RDR6 (Figure 7). In S-PTGS, where WT and 16C *N.benthamiana* inoculated with FL-GFP and 5´GFP, respectively, RDR6 is recruited to produce dsRNA from the aberrant GFP transcripts (Figure 5a). Rep protein suppressed the local silencing derived from RDR6 mediated dsRNA production. Therefore, 5´-GFP infiltrations do not lead to sRNA production when co-infiltrated with Rep. Unlike during S-PTGS, in IR induced PTGS, the hairpin transcript is already dsRNA, therefore RDR6 is not required for production of primary siRNAs, which leads to local silencing (Figure 5b) and in consequence BCTIV-Rep does not suppress IR-induced PGTS. It is noteworthy, however, that RDR6 is also indispensable for systemic silencing (Dalakouras et al, 2020). While a model where Rep interferes with RDR6 activity can explain our current observations, further experiments is needed to prove direct or indirect Rep and RDR6 interaction.

Moreover, the Rep protein of WDV has been functionally characterized. Truncations of WDV-Rep at the N terminus (9 amino acids) and the C-terminus (30 amino acids) did not affect the silencing suppression function and N-terminus was critical for necrotic phenotype. On the other hand, we have further characterized BCTIV-Rep with truncating domains on both the N and the C terminus. In the line with previous findings in WDV, pathogenicity determinant domain of BCTIV-Rep is also located on the N-terminus. However, we found that all truncated Rep proteins we produced, did not maintain the suppression of silencing phenotype of BCTIV-Rep.

Conclusion

In conclusion, we determined the BCTIV-Rep and -V2 as viral suppressors of RNA silencing. We showed that Rep reduces the siRNA accumulation mediated by RDR6 activity upon transient and stable expression of the target gene. On the other hand, BCTIV-V2 protein also has S-PTGS suppression activity only if GFP-FL is also transiently expressed, which is similar to other geminivirus V2 proteins and TBSV-P19.

Statement of Conflict.

The authors declare no conflict of interest.

Data Availability Statement

The coding sequences of the genes will be provided upon request.

Author Contributions

OE, GK, MW, and VVU designed the project. SE, AB, ZY conducted experiments. SE, VVU, and OE analyzed the data, VVU, GK, and SE wrote the manuscript. All authors analyzed the data and reviewed the manuscript. VVU supervised the study.

Funding

This study was financially supported by grants by the Federal Ministry of Education and Research (BMBF) Grant 03180531.

Acknowledgements

We thank Epi-Uslu Lab members at RLP AgroScience GmbH for the careful revision of the data and the manuscript.

References:

Ahn, J. W., Lee, J. S., Davarpanah, S. J., Jeon, J. H., Park, Y. Il, Liu, J. R., & Jeong, W. J. (2011). Host-dependent suppression of RNA silencing mediated by the viral suppressor p19 in potato. *Planta*, *234*(5), 1065–1072. https://doi.org/10.1007/S00425-011-1465-1/FIGURES/6

Anabestani, A., Behjatnia, S. A. A., Izadpanah, K., Tabein, S., & Accotto, G. P. (2017). Seed Transmission of Beet Curly Top Virus and Beet Curly Top Iran Virus in a Local Cultivar of Petunia in Iran. *Viruses*, *9*(10). https://doi.org/10.3390/V9100299

Baulcombe, D. (2004). RNA silencing in plants. *Nature 2004 431:7006*, *431*(7006), 356–363. https://doi.org/10.1038/nature02874

Bozorgi, N., Heydarnejad, J., Kamali, M., & Massumi, H. (2017). Splicing features in the expression of the complementary-sense genes of Beet curly top Iran virus. *Virus Genes*, *53*(2), 323–327. https://doi.org/10.1007/S11262-016-1422-Y

Dalakouras, A., Lauter, A., Bassler, A., Krczal, G., & Wassenegger, M. (2019). Transient expression of intron-containing transgenes generates non-spliced aberrant pre-mRNAs that are processed into siRNAs. *Planta*, *249*(2), 457–468. https://doi.org/10.1007/S00425-018-3015-6/FIGURES/8

Dunoyer, P., Himber, C., & Voinnet, O. (2005). DICER-LIKE 4 is required for RNA interference and produces the 21-nucleotide small interfering RNA component of the plant cell-to-cell silencing signal. *Nature Genetics*, *37*(12), 1356–1360. https://doi.org/10.1038/NG1675

Ebrahimi, S., Eini, O., Koolivand, D., & Varrelmann, M. (2022). The Rep and C1 of Beet curly top Iran virus represent pathogenicity factors and induce hypersensitive response in Nicotiana benthamiana plants. *Virus Genes*. https://doi.org/10.1007/S11262-022-01927-3

Eini, O., Sahraei, G. E., Ali, S., & Behjatnia, A. (2016). Molecular characterization and construction of an infectious clone of a pepper isolate of Beet curly top Iran virus. *Molecular Biology Research Communications*, *5*(2), 101. /pmc/articles/PMC5219900/

Feng, M., Zuo, D., Jiang, X., Li, S., Chen, J., Jiang, L., Zhou, X., & Jiang, T. (2018). Identification of Strawberry vein banding virus encoded P6 as an RNA silencing suppressor. *Virology*, *520*, 103–110. https://doi.org/10.1016/J.VIROL.2018.05.003

Haas, G., Azevedo, J., Moissiard, G., Geldreich, A., Himber, C., Bureau, M., Fukuhara, T., Keller, M., & Voinnet, O. (2008). Nuclear import of CaMV P6 is required for infection and suppression of the RNA silencing factor DRB4. *The EMBO Journal*, *27*(15), 2102–2112. https://doi.org/10.1038/EMBOJ.2008.129

Hanley-Bowdoin, L., Bejarano, E. R., Robertson, D., & Mansoor, S. (2013). Geminiviruses: masters at redirecting and reprogramming plant processes. *Nature Reviews. Microbiology*, *11*(11), 777–788. https://doi.org/10.1038/NRMICRO3117

Heydarnejad, J., Keyvani, N., Razavinejad, S., Massumi, H., & Varsani, A. (2013). Fulfilling Koch's postulates for beet curly top Iran virus and proposal for consideration of new genus in the family Geminiviridae. *Archives of Virology*, *158*(2), 435–443. https://doi.org/10.1007/S00705-012-1485-6

Himber, C., Dunoyer, P., Moissiard, G., Ritzenthaler, C., & Voinnet, O. (2003). Transitivity-dependent and -independent cell-to-cell movement of RNA silencing. *The EMBO Journal*, *22*(17), 4523–4533. https://doi.org/10.1093/EMBOJ/CDG431

Iki, T., Tschopp, M. A., & Voinnet, O. (2017). Biochemical and genetic functional dissection of the P38 viral suppressor of RNA silencing. *RNA (New York, N.Y.)*, *23*(5), 639–654. https://doi.org/10.1261/RNA.060434.116

Kalantidis, K., Schumacher, H. T., Alexiadis, T., & Helm, J. M. (2008). RNA silencing movement in plants. *Biology of the Cell*, *100*(1), 13–26. https://doi.org/10.1042/BC20070079

Kasschau, K. D., & Carrington, J. C. (1998). A counterdefensive strategy of plant viruses: suppression of posttranscriptional gene silencing. *Cell*, *95*(4), 461–470. https://doi.org/10.1016/S0092-8674(00)81614-1

Kotlizky, G., Boulton, M. I., Pitaksutheepong, C., Davies, J. W., & Epel, B. L. (2000). Intracellular and Intercellular Movement of Maize Streak Geminivirus V1 and V2 Proteins Transiently Expressed as Green Fluorescent Protein Fusions. *Virology*, *274*(1), 32–38. https://doi.org/10.1006/VIRO.2000.0415

Kumar, R. V. (2019). Plant antiviral immunity against geminiviruses and viral counter-defense for survival. *Frontiers in Microbiology*, *10*(JUN), 1460. https://doi.org/10.3389/FMICB.2019.01460/BIBTEX

Liu, Y., Jin, W., Wang, L., & Wang, X. (2014). Replication-associated proteins encoded by Wheat dwarf virus act as RNA silencing suppressors. *Virus Research*, *190*, 34–39. https://doi.org/10.1016/J.VIRUSRES.2014.06.014

Lu, R., Folimonov, A., Shintaku, M., Li, W. X., Falk, B. W., Dawson, W. O., & Ding, S. W. (2004). Three distinct suppressors of RNA silencing encoded by a 20-kb viral RNA genome. *Proceedings of the National Academy of Sciences of the United States of America*, *101*(44), 15742–15747. https://doi.org/10.1073/PNAS.0404940101

Luna, A. P., Rodríguez-Negrete, E. A., Morilla, G., Wang, L., Lozano-Durán, R., Castillo, A. G., & Bejarano, E. R. (2017). V2 from a curtovirus is a suppressor of post-transcriptional gene silencing. *The Journal of General Virology*, *98*(10), 2607–2614. https://doi.org/10.1099/JGV.0.000933

Martín-Hernández, A. M., & Baulcombe, D. C. (2008). Tobacco rattle virus 16-kilodalton protein encodes a suppressor of RNA silencing that allows transient viral entry in meristems. *Journal of Virology*, *82*(8), 4064–4071. https://doi.org/10.1128/JVI.02438-07

Parent, J. S., Jauvion, V., Bouché, N., Béclin, C., Hachet, M., Zytnicki, M., & Vaucheret, H. (2015). Post-transcriptional gene silencing triggered by sense transgenes involves uncapped antisense RNA and differs from silencing intentionally triggered by antisense transgenes. *Nucleic Acids Research*, *43*(17), 8464–8475. https://doi.org/10.1093/NAR/GKV753

Ruhel, R., & Chakraborty, S. (2019). Multifunctional roles of geminivirus encoded replication initiator protein. *Virusdisease*, *30*(1), 66–73. https://doi.org/10.1007/S13337-018-0458-0

Saeed, M., Briddon, R. W., Dalakouras, A., Krczal, G., & Wassenegger, M. (2015). Functional Analysis of Cotton Leaf Curl Kokhran Virus/Cotton Leaf Curl Multan Betasatellite RNA Silencing Suppressors. *Biology 2015, Vol. 4, Pages 697-714*, *4*(4), 697–714. https://doi.org/10.3390/BIOLOGY4040697

Silhavy, D., Molnár, A., Lucioli, A., Szittya, G., Hornyik, C., Tavazza, M., & Burgyán, J. (2002). A viral protein suppresses RNA silencing and binds silencing-generated, 21- to 25-nucleotide double-stranded RNAs. *The EMBO Journal*, *21*(12), 3070–3080. https://doi.org/10.1093/EMBOJ/CDF312

Stanley, J., & Latham, J. R. (1992). A symptom variant of beet curly top geminivirus produced by mutation of open reading frame C4. *Virology*, *190*(1), 506–509. https://doi.org/10.1016/0042-6822(92)91243-N

Vargason, J. M., Szittya, G., Burgyán, J., & Tanaka Hall, T. M. (2003). Size selective recognition of siRNA by an RNA silencing suppressor. *Cell*, *115*(7), 799–811. https://doi.org/10.1016/S0092-8674(03)00984-X

Voinnet, O. (2022). Revisiting small RNA movement in plants. In *Nature Reviews Molecular Cell Biology* (Vol. 23, Issue 3, pp. 163–164). https://doi.org/10.1038/s41580-022-00455-0

Voinnet, O., Rivas, S., Mestre, P., & Baulcombe, D. (2003). An enhanced transient expression system in plants based on suppression of gene silencing by the p19 protein of tomato bushy stunt virus. *The Plant Journal : For Cell and Molecular Biology*, *33*(5), 949–956. https://doi.org/10.1046/J.1365-313X.2003.01676.X

Wang, Y., Dang, M., Hou, H., Mei, Y., Qian, Y., & Zhou, X. (2014). Identification of an RNA silencing suppressor encoded by a mastrevirus. *The Journal of General Virology*, *95*(Pt 9), 2082–2088. https://doi.org/10.1099/VIR.0.064246-0

Yazdi, H. R. B., Heydarnejad, J., & Massumi, H. (2008). Genome characterization and genetic diversity of beet curly top Iran virus: a geminivirus with a novel nonanucleotide. *Virus Genes*, *36*(3), 539–545. https://doi.org/10.1007/S11262-008-0224-2

Ye, K., Malinina, L., & Patel, D. J. (2003). Recognition of small interfering RNA by a viral suppressor of RNA silencing. *Nature*, *426*(6968), 874. https://doi.org/10.1038/NATURE02213

Zhang, J., Dong, J., Xu, Y., & Wu, J. (2012). V2 protein encoded by Tomato yellow leaf curl China virus is an RNA silencing suppressor. *Virus Research*, *163*(1), 51–58. https://doi.org/10.1016/J.VIRUSRES.2011.08.009

Zhang, X.-F., Guo, J., Zhang, X., Meulia, T., Paul, P., Madden, L. V, Li, D., & Qu, F. (2015). Random Plant Viral Variants Attain Temporal Advantages During Systemic Infections and in Turn Resist other Variants of the Same Virus OPEN. *Nature Publishing Group*. https://doi.org/10.1038/srep15346

Zrachya, A., Glick, E., Levy, Y., Arazi, T., Citovsky, V., & Gafni, Y. (2006). *Suppressor of RNA silencing encoded by Tomato yellow leaf curl virus-Israel*. https://doi.org/10.1016/j.virol.2006.08.016

Table 1: Primers used for BCTIV cloning:

Internal Reference	Primer Name	Sequence
2116	**Rep-noIntJ-noC2-R**	AACAggatccTTAGAAATATATATTTTGTTCCG
2117	**Rep-IntJ-noC2-R**	AACAggatccTTAATAGTGGTGTCGGCCTAGAGAT
2118	**Rep-intJ-C2(PNLV)-R**	AACAggatccTTAAATGACTAAGTTTGGTTTAT
2119	**Rep-intJ-C2(CMSES)-R**	AACAggatccTTAAGATTCACTCATACAAGGTATCC
2120	**Rep-dN(1)-Fw**	AACActcgagATGACGAGCCCTAGAACATTTGGA
2121	**Rep-ddN(2) -Fw**	GAATTCctcgagATGTCCATTCTATCCTTCGCCAAC
2122	**Rep-intF(3) -Fw**	GAATTCctcgagATGGAGCCAGACAACAGACCAGTC
2095	**BCTIVtoG104f**	AACActcgagTGGAGAGGATCGATTAGGAG
2096	**BCTIVtoG104r**	AACAggatccCTTATCTGGGAACTACTCACAC
2098	**BCTIV_V2-rv**	ggatccGAAACTGTCCTCCCACCGGT
2099	**BCTIV_to_G104_V2-F**	AACAGGATCCATGGTACCTTTCAGAGTGAGCG

Figure Legends

Figure 1| Screening of BCTIV genes for VSR activity a) GFP expressing 16C *N.benthamiana* leaves were co-infiltrated with S-PTGS inducer 5'-GFP and a single BCTIV gene for each experiment. At 6dpi, if 5'-GFP leads to red sectors under the UV lamp, it suggests that the VSR activity of the co-infiltrated gene is negligible. However, if the infiltrated sector remains green under UV lamp, it shows VSR activity for the gene of interest. b) Whole plant photos of the co-infiltrated plants were taken under UV light by a DLSR camera at 6dpi. Representative images of at least three biological replicates are provided. c) High-resolution images of the leaves infiltrated by 5'-GFP and C1, C2, C4, C5, Rep, V1, V2, V3, and V4 are obtained at 50µm/pixel using green and far-red channels of PharosFX™ imager. Green (GFP) and far-red channels (chlorophyll) are merged using FIJI. d) Non-vasculature sectors of the high-resolution leaf images are quantified based on GFP intensity using the rectangle tool in FIJI. At least three leaves and multiple areas per leaf were quantified. The values are plotted by the online BoxPlotR tool by Shiny Lab. One-way ANOVA statistical test shows significance at $p<0.05$. e)

571 Top panel shows northern blot results using a radioactively labeled GFP probe. 5'-GFP serves as a
572 low GFP expression control and a 16C-untreated sample shows high-abundance GFP mRNA control.
573 rRNA is a loading control for the upper panel, obtained by agarose gel electrophoresis using
574 ethidium bromide staining. f) Top panel shows small RNA Northern blot using a radioactively labeled
575 GFP probe. The bands correspond to 21 and 24 nt long siRNAs. 5'-GFP serves as a highly abundant
576 siRNA control and 16C-untreated serves as a clean negative control. The lower panel is the small
577 RNA Northern blot by using U6 RNA labeling as a control for RNA loading. U6 RNA labeling took place
578 on the same membrane given in the panel above, after stripping.

579

580 **Figure 2|BCTIV-Rep and BCTIV-V2 genes repress S-PTGS upon transient expression of GFP** a) S-
581 PTGS inducing FL-GFP is co-infiltrated with C1, C2, Rep, and V2 of BCTIV on wt *N.benthamiana*. Upon
582 VSR activity, FL-GFP agroinfiltration is expected to show high GFP fluorescence under UV light. b)
583 Whole plant photos of the co-infiltrated plants taken by a DLSR camera at 6dpi are shown. TBSV-p19
584 co-infiltration with FL-GFP is used as a positive control for very high GFP expression and FL-GFP
585 single infiltration serves as a low GFP expression control. c) High-resolution images of the leaves
586 infiltrated by FL-GFP and virus genes are obtained at 50µm/pixel using green and far-red channels of
587 PharosFX™ imager. Green (GFP) and far-red channels (chlorophyll) are merged using FIJI. d)
588 Infiltrated areas in the leaves are quantified based on GFP intensity using the rectangle tool in FIJI. At
589 least three leaves and multiple areas per leaf were quantified. The values are plotted by the online
590 BoxPlotR tool by Shiny Lab. One-way ANOVA statistical test shows significance at $p<0.05$. e) The top
591 panel is the Western blot result, showing the abundance of GFP protein in the co-infiltrated sections
592 of the very same leaves shown in c. the lower panel is the Rubisco band in the Coomassie staining as
593 a loading control for the Western blot. Since the assay is performed on wt *N.benthamiana,* it allows
594 quantification of absolute changes in GFP level, and therefore a reliable comparison of image
595 quantifications and protein abundance in Western blot f) FL-GFP is co-infiltrated with p19, V2, and
596 Rep. Representative images from at least two plants and multiple leaves are provided. g) The GFP
597 level quantification of the co-infiltrated sectors normalized to the non-infiltrated sectors of the
598 treated leaves using FIJI. One-Way ANOVA test has been conducted with a threshold of $p<0.05$.

599

600 **Figure 3|Neither BCTIV-Rep nor BCTIV-V2 can suppress PTGS induced by GFP-IR.** a) PTGS inducing
601 GFP-IR is co-infiltrated with C1, C2, Rep, and V2 of BCTIV on 16C *N.benthamiana*. Upon VSR activity,
602 GFP-IR agroinfiltrated sectors are expected to retain high GFP fluorescence under UV light. b) Whole
603 plant photos of the co-infiltrated plants taken under UV light by a DLSR camera at 6dpi are shown.
604 Representative images of at least three biological replicates are provided. c) High-resolution images
605 of the leaves infiltrated by GFP-IR and C1, C2, Rep, V2, and p19 are obtained at 50µm/pixel using
606 green and far-red channels of PharosFX™ imager. Green (GFP) and far-red channels (chlorophyll) are
607 merged using FIJI. d) Non-vasculature sectors of the high-resolution leaf images are quantified based
608 on GFP intensity using the rectangle tool in FIJI. At least three leaves and multiple areas per leaf
609 were quantified. The values are plotted by the online BoxPlotR tool by Shiny Lab. One-way ANOVA
610 statistical test shows significance at $p<0.05$. e) Top panel shows northern blot results using a
611 radioactively labeled GFP probe. GFP-IR serves as a low GFP expression control and a 16C-untreated
612 sample shows high-abundance GFP mRNA control. rRNA is a loading control for the upper panel,
613 obtained by agarose gel electrophoresis using ethidium bromide staining. f) Top panel shows small-
614 RNA-Northern blot using a radioactively labeled GFP probe. The bands correspond to 21 and 24 nt
615 long siRNAs. GFP-IR serves as a highly abundant siRNA control and 16C-untreated serves as a
616 negative control. The lower panel is the small RNA Northern blot by using U6 RNA labeling as a

control for RNA loading. U6 RNA labeling took place on the same membrane given in the panel above, after stripping. g) A minimum of twelve 16C *N.benthamiana* used for GFP-IR co-infiltration with VSR candidates are followed for at least until 14dpi. The images of the whole plant are taken using a DSLR Camera under UV light and one representative image per treatment is given. h) The total number of co-infiltrated plants, remaining healthy at 14dpi is provided on the top row, and the number of plants showing systemic silencing in at least two leaves is given the bottom row.

Figure 4| BCTIV-Rep or -V2 does not block the short-range spreading of silencing upon IR induced PTGS. a-g) 16C plants are infiltrated with GFP-FL and GFP-IR only(a), GFP-FL, GFP-IR, and TBSV-p19(b), GFP-FL, GFP-IR, and BCTIV-V2(c), GFP-FL, GFP-IR, and BCTIV-Rep(d). The images are overlay of green and far-red channels, acquired by PharosFX™ imager at 5.25dpi. The close-up on the right highlights the red sector around the infiltration area. b-h) GFP intensity profile of a 10pixel-wide line depicted on the close-up image on the right. Y-axis gives the intensity of the GFP in gray value, X-axis is the distance (in mm) of the spot to the * end of the line given. The left end of the x-axis is the # end of the line. The red dotted line indicates the distance of the short-term spread of local silencing in mm. i) The GFP intensity measurement of infiltrated non-vasculature areas is normalized to their non-infiltrated areas in the same leaf. 16C + GFP-FL infiltrated measurements are taken from Figure 1g for comparison. The corresponding measurement number is given below the bar. One-Way ANOVA test has been conducted with a threshold of $p<0.05$.

Figure 5| Multiple domains are needed for VSR activity of BCTIV-Rep. a) GFP expressing 16C *N.benthamiana* leaves were co-infiltrated with S-PTGS inducer 5'-GFP and a single BCTIV-Rep truncation in each experiment. At 6dpi, if 5'-GFP leads to red sectors under the UV lamp, it suggests that the VSR activity of the co-infiltrated gene is negligible. However, if the infiltrated sector remains green under UV lamp, it shows VSR activity for the gene of interest. b) Whole plant photos of the co-infiltrated plants were taken under UV light by a DLSR camera at 6dpi. Representative images of the two biological replicates are provided for each co-infiltration. c) High-resolution images of the co-infiltrated leaves are obtained at 50µm/pixel using green and far-red channels of PharosFX™ imager. Green (GFP) and far-red channels (chlorophyll) are merged using FIJI. d) The GFP intensity of the non-vasculature sectors of the high-resolution leaf images are normalized to the non-infiltrated side of the same leaf. At least two leaves and multiple areas per leaf were quantified. The values are plotted by the online BoxPlotR tool by Shiny Lab. One-way ANOVA statistical test shows significance at $p<0.05$.

Figure 6| Proposed model for the mode of action of BCTIV-Rep VSR activity. a) S-PTGS is triggered by the RDR6-driven dsRNA synthesis using aberrant RNA (abRNA) as a template. Both 5'-GFP and GFP-FL dsRNAs are cleaved into sRNAs by DCLs. The sRNAs are loaded onto AGO proteins for cleavage of the target GFP mRNA. In the presence of Rep, S-PTGS mechanism does not function. GFP mRNA Northern blot shows that Rep represses the cleavage of GFP mRNA by S-PTGS inducer. Moreover, sRNA Northern Blot showed that Rep also suppresses the production of sRNAs. Therefore, Rep-VSR activity should be associated by the inhibition of DCL or RDR6 activity b) PTGS induced by GFP-IR shows that Rep cannot block the local silencing, triggered by DCL cleave of the GFP-IR, suggesting that Rep does not interfere with the DCL activity, which leaves RDR6 as the only possible target of Rep. Moreover, Rep still reduces the sRNAs produced GFP-IR, suggesting that the

propagation of the sRNA production (positive feedback loop) by RDR6 is mitigated by Rep, pointing out to the interaction between Rep and RDR6.

FIGURES:

FIGURE 1

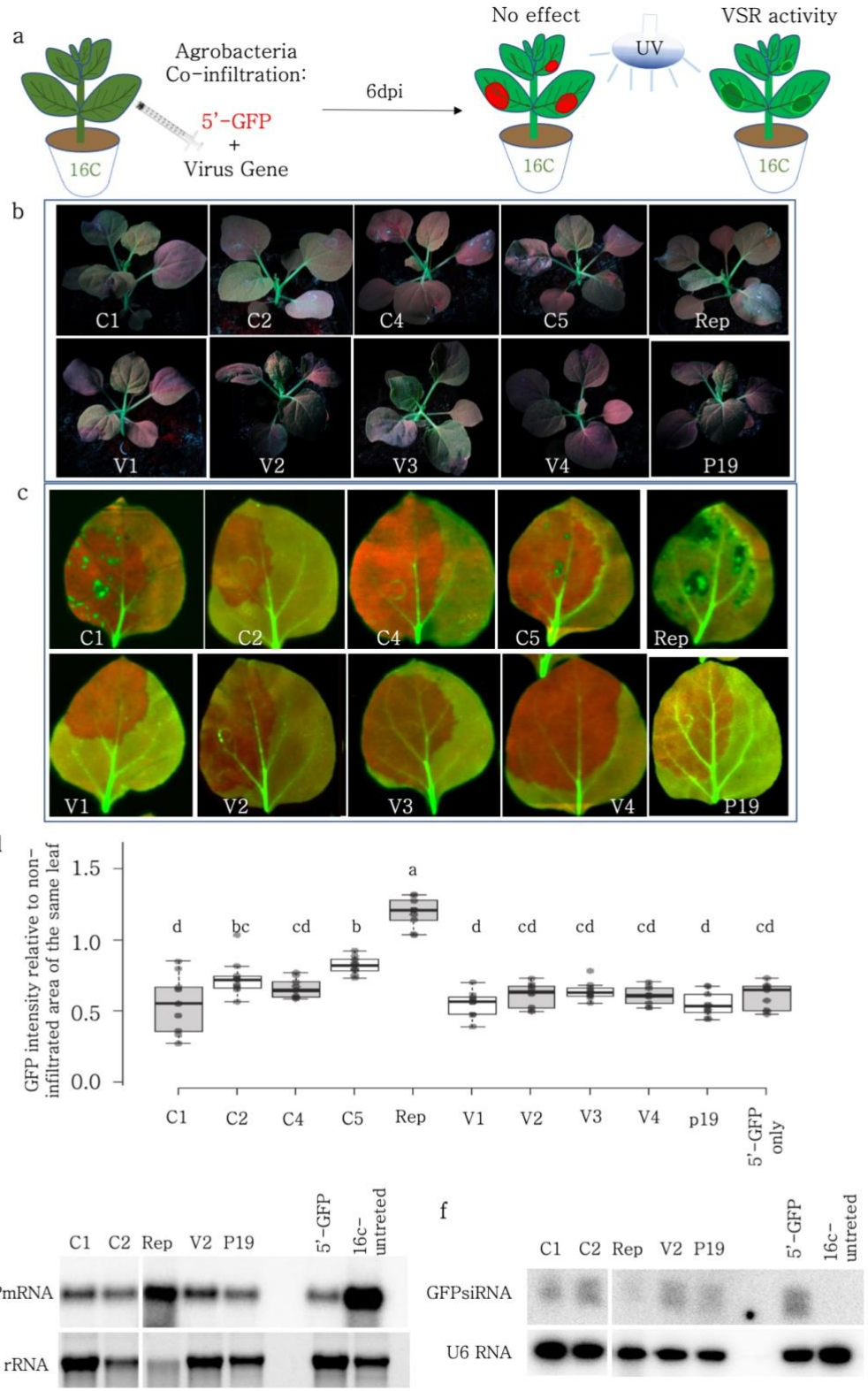

FIGURE 2

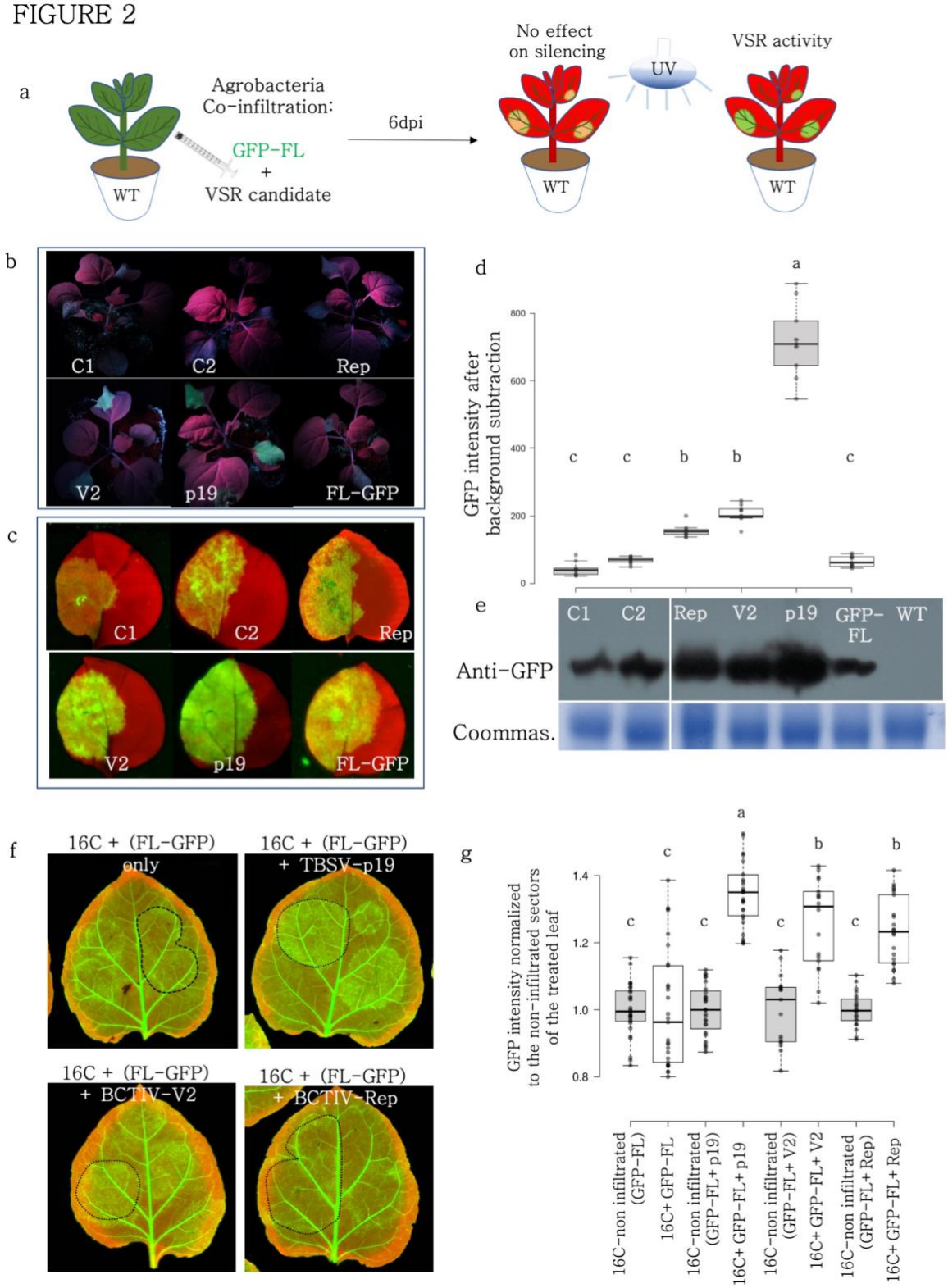
a
Agrobacteria
Co-infiltration:
GFP-FL
+
VSR candidate
WT
6dpi
No effect
on silencing
UV
VSR activity
WT
WT
b
C1
C2
Rep
V2
p19
FL-GFP
c
C1
C2
Rep
V2
p19
FL-GFP
d
GFP intensity after
background subtraction
800
600
400
200
0
a
c
c
b
b
c
e
C1
C2
Rep
V2
p19
GFP-
FL
WT
Anti-GFP
Coommas.
f
16C + (FL-GFP)
only
16C + (FL-GFP)
+ TBSV-p19
16C + (FL-GFP)
+ BCTIV-V2
16C + (FL-GFP)
+ BCTIV-Rep
g
GFP intensity normalized
to the non-infiltrated sectors
of the treated leaf
1.4
1.2
1.0
0.8
a
c
b
b
c
c
c
c
16C-non infiltrated
(GFP-FL)
16C+ GFP-FL
16C-non infiltrated
(GFP-FL+ p19)
16C+ GFP-FL+ p19
16C-non infiltrated
(GFP-FL+ V2)
16C+ GFP-FL+ V2
16C-non infiltrated
(GFP-FL+ Rep)
16C+ GFP-FL+ Rep

666

FIGURE 3

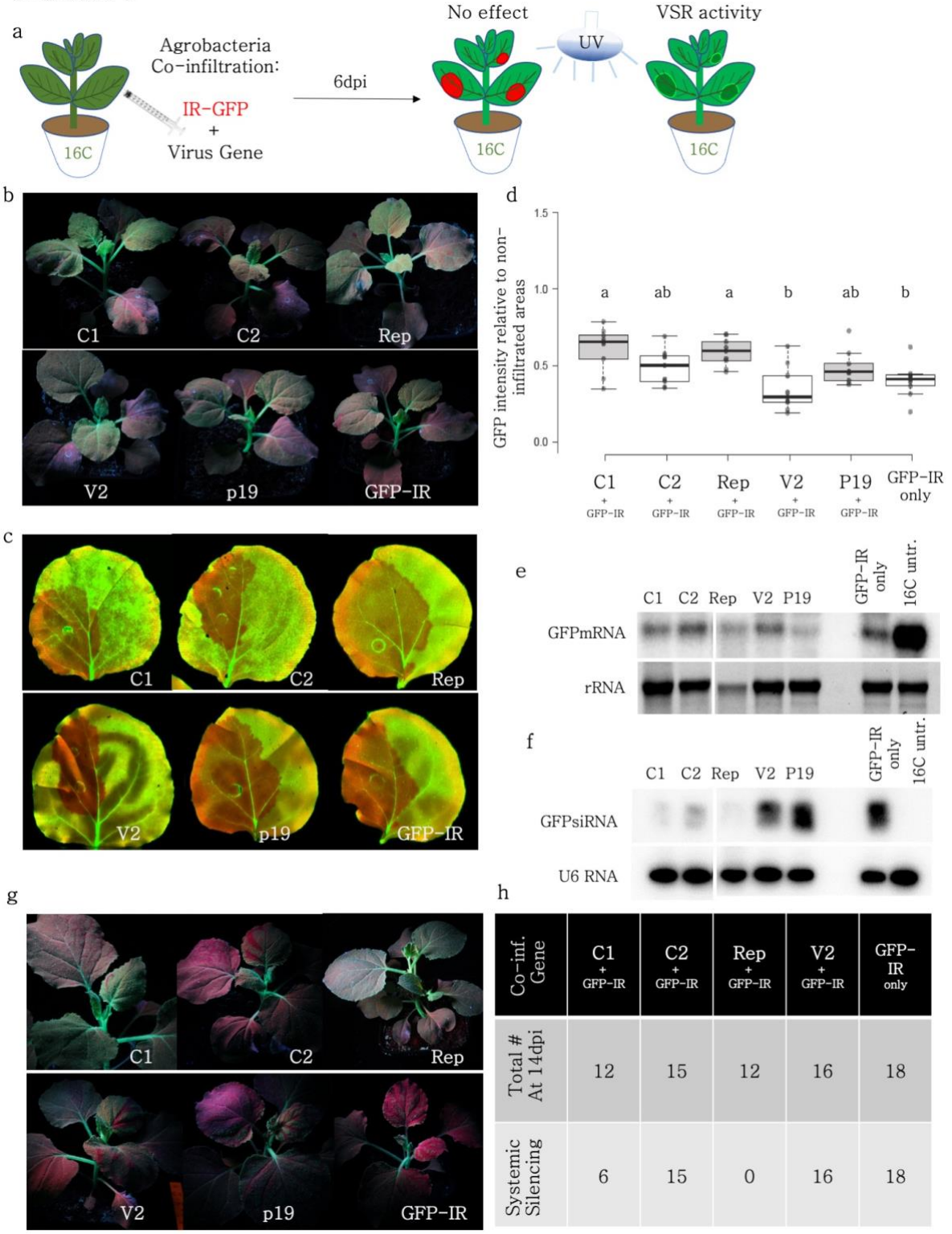

Co-inf. Gene	C1 + GFP-IR	C2 + GFP-IR	Rep + GFP-IR	V2 + GFP-IR	GFP-IR only
Total # At 14dpi	12	15	12	16	18
Systemic Silencing	6	15	0	16	18

667

FIGURE 4

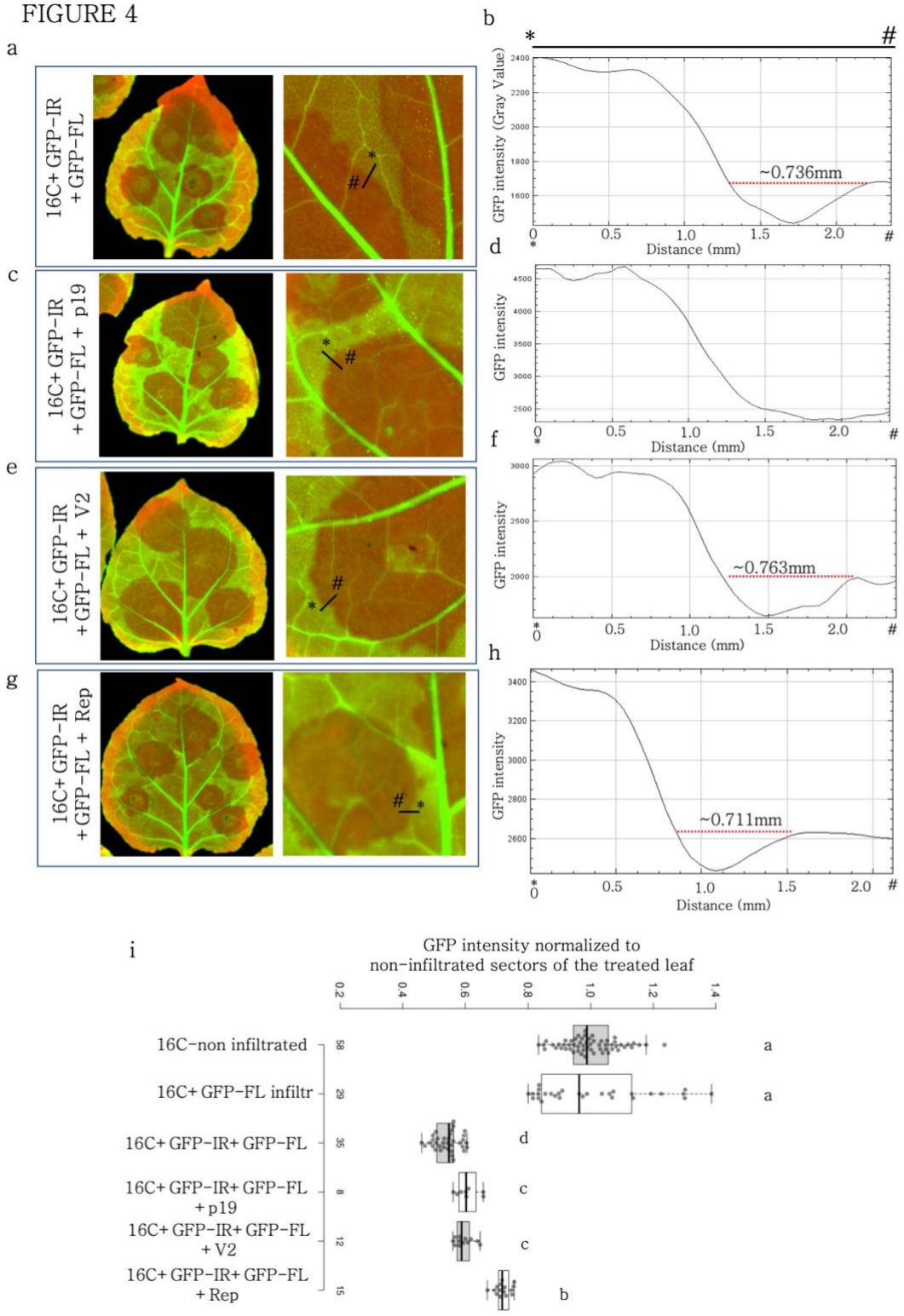
a
16C+ GFP-IR + GFP-FL
b
~0.736mm
GFP intensity (Gray Value)
Distance (mm)
c
16C+ GFP-IR + GFP-FL + p19
d
GFP intensity
Distance (mm)
e
16C+ GFP-IR + GFP-FL + V2
f
~0.763mm
GFP intensity
Distance (mm)
g
16C+ GFP-IR + GFP-FL + Rep
h
~0.711mm
GFP intensity
Distance (mm)

i
GFP intensity normalized to non-infiltrated sectors of the treated leaf
16C-non infiltrated
16C+ GFP-FL infiltr
16C+ GFP-IR+ GFP-FL
16C+ GFP-IR+ GFP-FL + p19
16C+ GFP-IR+ GFP-FL + V2
16C+ GFP-IR+ GFP-FL + Rep
58
29
35
8
12
15
a
a
d
c
c
b

668

FIGURE 5

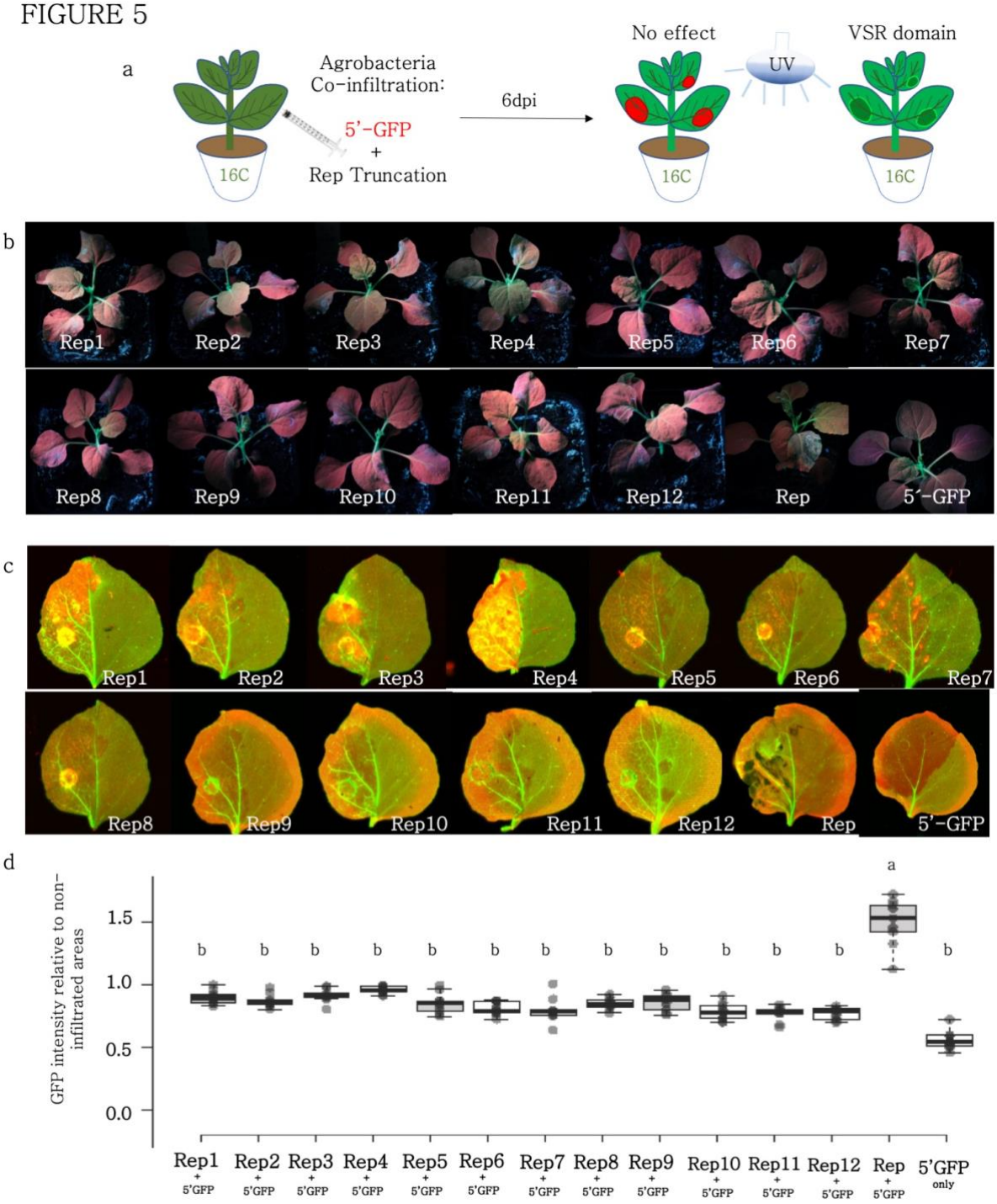
a
Agrobacteria
Co-infiltration:
5'-GFP
+
Rep Truncation
6dpi
No effect
UV
VSR domain
16C
16C
16C
b
Rep1
Rep2
Rep3
Rep4
Rep5
Rep6
Rep7
Rep8
Rep9
Rep10
Rep11
Rep12
Rep
5'-GFP
c
Rep1
Rep2
Rep3
Rep4
Rep5
Rep6
Rep7
Rep8
Rep9
Rep10
Rep11
Rep12
Rep
5'-GFP
d
GFP intensity relative to non-infiltrated areas
1.5
1.0
0.5
0.0
a
b
Rep1 + 5'GFP
Rep2 + 5'GFP
Rep3 + 5'GFP
Rep4 + 5'GFP
Rep5 + 5'GFP
Rep6 + 5'GFP
Rep7 + 5'GFP
Rep8 + 5'GFP
Rep9 + 5'GFP
Rep10 + 5'GFP
Rep11 + 5'GFP
Rep12 + 5'GFP
Rep + 5'GFP
5'GFP only

669

FIGURE 6

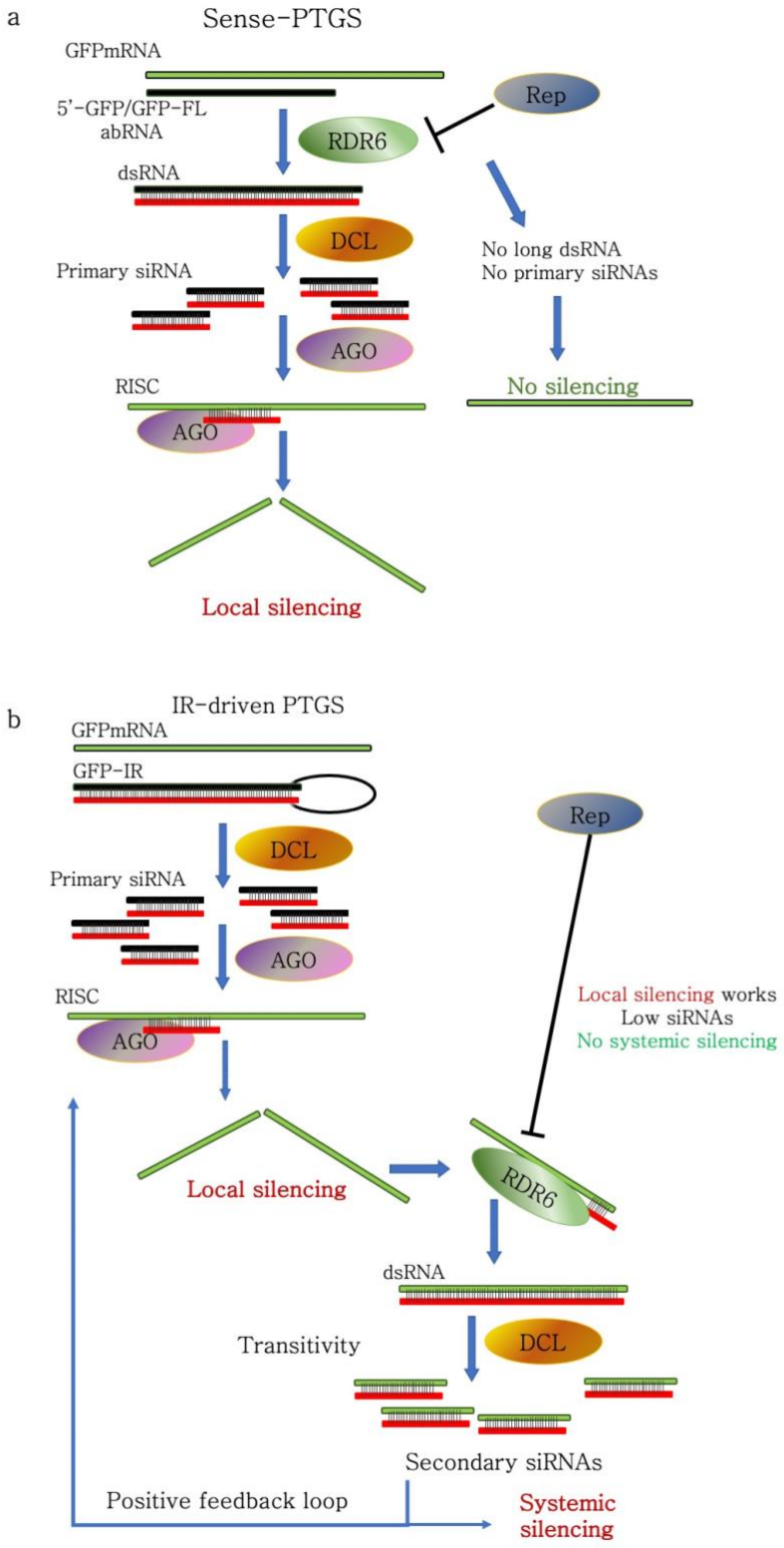
a
Sense-PTGS
GFPmRNA
5'-GFP/GFP-FL
abRNA
Rep
RDR6
dsRNA
DCL
Primary siRNA
No long dsRNA
No primary siRNAs
AGO
RISC
No silencing
AGO
Local silencing
b
IR-driven PTGS
GFPmRNA
GFP-IR
Rep
DCL
Primary siRNA
AGO
RISC
Local silencing works
Low siRNAs
No systemic silencing
AGO
Local silencing
RDR6
dsRNA
Transitivity
DCL
Secondary siRNAs
Positive feedback loop
Systemic
silencing

670